

Transmembrane localization of *cis*-isomers of zeaxanthin in the host dimyristoylphosphatidylcholine bilayer membrane

Justyna Widomska, Witold K. Subczynski *

Department of Biophysics, Medical College of Wisconsin, 8701 Watertown Plank Road, Milwaukee, WI 53226, USA

Received 29 June 2007; received in revised form 2 August 2007; accepted 16 August 2007

Available online 6 September 2007

Abstract

The effects of the 9-*cis* and 13-*cis* isomers of zeaxanthin on the molecular organization and dynamics of dimyristoylphosphatidylcholine (DMPC) membranes were investigated using conventional and saturation recovery EPR observations of the 1-palmitoyl-2-(14-doxylstearoyl) phosphatidylcholine (14-PC) spin label. The results were compared with the effects caused by the all-*trans* isomer of zeaxanthin. Effects on membrane fluidity, order, hydrophobicity, and the oxygen transport parameter were monitored at the center of the fluid phase DMPC membrane. The local diffusion-solubility product of oxygen molecules (oxygen transport parameter) in the membrane center, studied by saturation-recovery EPR, decreased by 47% and 27% by including 10 mol% 13-*cis* and 9-*cis* zeaxanthin, respectively; whereas, incorporation of all-*trans* zeaxanthin decreased this parameter by only 11%. At a zeaxanthin-to-DMPC mole ratio of 1:9, all investigated isomers decreased the membrane fluidity and increased the alkyl chain order in the membrane center. They also increased the hydrophobicity of the membrane interior. The effects of these isomers of zeaxanthin on the membrane properties mentioned above increase as: all-*trans* < 9-*cis* ≤ 13-*cis*. Obtained results suggest that the investigated *cis*-isomers of zeaxanthin, similar to the all-*trans* isomer, are located in the membrane interior, adopting transmembrane orientation with the polar terminal hydroxyl groups located in the opposite leaflets of the bilayer. However, the existence of the second pool of *cis*-zeaxanthin molecules located in the one leaflet and anchored by the terminal hydroxyl groups in the same polar headgroup region cannot be completely ruled out.

© 2007 Elsevier B.V. All rights reserved.

Keywords: *cis*-Zeaxanthin; Xanthophyll; Carotenoid; Lipid bilayer; Spin labeling; EPR

1. Introduction

The heterogeneity of carotenoids is greatly increased by the existence of their geometrical isomers. The polyene-chain double bonds present in carotenoids can exist in mono-*cis*, poly-*cis*, or all-*trans* configurations; however, the vast majority of naturally occurring carotenoids exist in all-*trans* conformations. In organisms that can synthesize carotenoids (lower organisms and plants), the geometrical isomers of carotenoids have specific distributions and functions in their photobiology. For example, for *Rhodospirillum rubrum* the all-*trans* isomer of spirilloxanthin is selected by the light-harvesting complexes, whereas the 15-*cis* isomer is selected by the reaction centers [1]. In the photosynthetic tissues of plants, the 9'-*cis* form of neoxanthin (but not the all-*trans* form) was found in the chloroplasts of seed plants, ferns, mosses and green algae, which all contain chlorophylls *a* and *b*;

whereas, the all-*trans* form of neoxanthin was found only in non-photosynthetic organs [2]. It is uncertain, however, if similar specific distributions and functions of geometrical isomers exist in animals, including humans.

Animals cannot synthesize carotenoids, but obtain them from diet. Dietary carotenoids exist mostly as all-*trans* isomers, but *cis*-isomers (5-, 9-, 13-, and 15-*cis*) are also present in food in significant quantities. These *cis*-isomers of carotenoids have also been identified in human plasma [3,4]. Some papers suggest a different intestinal uptake of *trans*- and *cis*-isomers of β -carotene [5,6]. It also has been shown that *cis*-isomers of lycopene are better absorbed than all-*trans* isomers, and it has been suggested that this is because *cis*-isomers of lycopene are more soluble (more readily incorporated) in chylomicrons than all-*trans* isomers [7,8]. A significant difference between the amount of *cis*-isomers of xanthophylls in both a monkey's diet and a monkey's plasma also has been reported [9]. It should be noted that the zeaxanthin-to-lutein ratio in the plasma of monkeys is very similar to that of humans. The 9-*cis* isomer of both lutein

* Corresponding author. Tel.: +1 414 456 4038; fax: +1 414 456 6512.

E-mail address: subczyn@mcw.edu (W.K. Subczynski).

and zeaxanthin is generally present at a very low level in the plasma of monkeys, much lower than is present in their diet; however, for the 13-*cis* isomer, the situation is reversed.

We are especially interested in the localization of macular xanthophylls in lipid bilayer membranes and their interaction with the membrane. All major macular xanthophylls – lutein, zeaxanthin, and *meso*-zeaxanthin – are dipolar, terminally dihydroxylated carotenoids. In the lipid bilayer membranes, all-*trans* isomers of these xanthophylls adopt transmembrane orientation with the polar terminal hydroxyl groups anchored in the polar headgroup region of the opposite leaflets of the bilayer [10–16]. The data demonstrate that lutein molecules can exist in two pools, one in which they accept transmembrane orien-

tation, and the other in which they accept orientation parallel to the membrane surface, with the polar terminal hydroxyl groups anchored in the polar headgroup region of the same leaflet of the bilayer [11]. Only lutein and zeaxanthin are selectively accumulated in membranes of the eye retina from blood plasma. Another macular xanthophyll, *meso*-zeaxanthin, is presumably formed from lutein in the retina [17,18].

In addition to the all-*trans* isomers, the *cis*-isomers of macular xanthophylls also were isolated from the human eye retina and characterized [19]. The 9-*cis* and 13-*cis* isomers of zeaxanthin were present in the greatest amounts [19]. It is commonly accepted that these *cis*-isomers are mainly produced directly in the eye retina under the intensive light exposure from

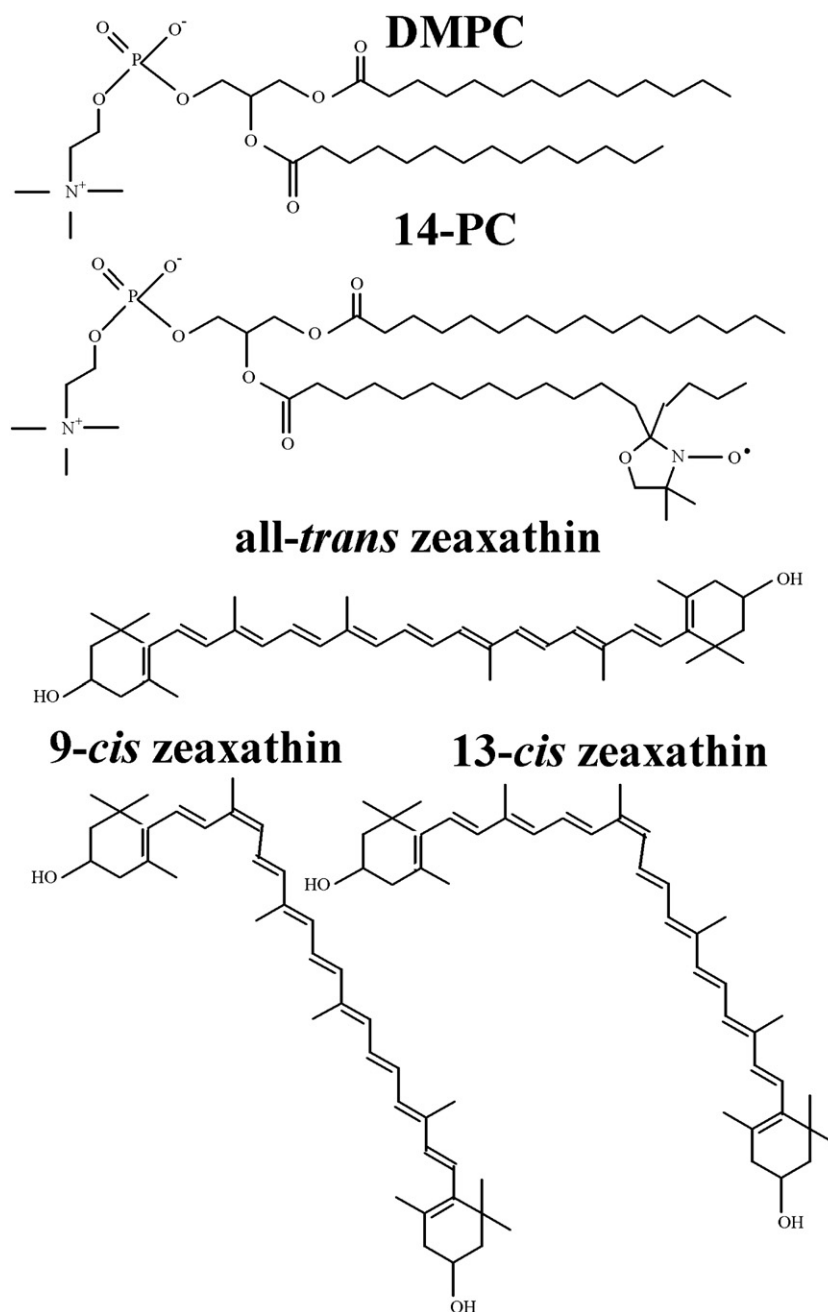


Fig. 1. The structures of all-*trans*, 9-*cis*, and 13-*cis* geometrical isomers of zeaxanthin together with the structure of DMPC and 14-PC spin label.

the all-*trans* isomers already selectively accumulated there from the blood plasma [20]. It is unknown if the *cis*-isomers are serving any function in the eye retina, or if they are only the products of light-induced isomerization. Also, their localization and orientation in the membrane were not investigated. Based on the molecular structure of the *cis*-isomers, localization of polar and hydrophobic parts of the molecule, and the “fit” to the membrane hydrophobic thickness, a model was proposed that placed the *cis*-isomers of zeaxanthin horizontally with respect to the plane of the membrane and with polar hydroxyl groups anchored in the same polar headgroup region (the same leaflet) of the bilayer (see Review [21]). However, there are no data that confirm or reject this model, and because of this we have undertaken measurements, using different EPR spin labeling approaches, to look at the effects of *cis*-isomers of zeaxanthin on different properties of the central region of the DMPC bilayer and compared them with those effects caused by the *trans*-isomer of zeaxanthin.

Zeaxanthin was chosen for these investigations because its interaction with membranes has been investigated in great details [10,22–25]. Additionally, zeaxanthin adopts only trans-membrane orientation in lipid bilayers [10,11,15,16] (including the DMPC bilayer [10]), which makes the interpretation of our results much simpler. The saturated phospholipid DMPC was chosen because the interaction of different carotenoids (especially macular xanthophylls) with the DMPC bilayer membrane also has been extensively investigated [10,22–26]. It is also convenient that the DMPC bilayer has the main phase transition at 23.6 °C, and, thus, it exists at physiological temperatures in the biologically relevant fluid phase. Additionally, the effects of xanthophylls on membrane properties, observed by the use of EPR spin labeling methods in saturated membranes, are much greater than those observed in unsaturated membranes [24]. Also, we think the measurements in the membrane center, not at or close to the membrane surface, can unequivocally confirm which orientation of the *cis*-isomers of zeaxanthin in the membrane is the most probable, horizontal or transmembrane (see also Discussion). Because of this we chose the 14-PC to place the nitroxide moiety of the spin label exactly at the center of the DMPC bilayer, possessing 14 carbon atoms in the alkyl chains. Our measurements indicate that in the DMPC bilayer the trans-membrane orientation of *cis*-isomers of zeaxanthin is prevalent; however, we cannot completely exclude the existence of the horizontal orientation.

2. Materials and methods

2.1. Materials

Synthetic crystalline all-*trans* zeaxanthin ((3*R*,3'*R*)- β , β -carotene-3,3'-diol) was purchased from CarotenNature (Lupsingen, Switzerland). 9-*cis* and 13-*cis* isomers of zeaxanthin were obtained as a product of iodine-catalyzed photo-conversion of the all-*trans* form following the procedure described by Molnar and Szablocs [27]. Isomeric forms of zeaxanthin were separated chromatographically on C-30-coated high-performance liquid chromatography (ProntSIL, length 250 mm, internal diameter: 4.6 mm). Solvent mixture of methyl tertiary butyl ether/methanol (5:95, v/v) was used as a mobile phase. The efficiency of this method was rather low, and amounts of available *cis*-isomers were limited. Dimyristoylphosphatidylcholine (DMPC), 1-palmitoyl-2-(14-doylestearoyl)

phosphatidylcholine (14-PC), and 1-palmitoyl-2-(5-doylestearoyl)phosphatidylcholine (5-PC) were obtained from Avanti Polar Lipids, Inc. (Alabaster, AL). Other chemicals of at least reagent grade were purchased from Aldrich (Milwaukee, WI). Chemical structures of geometrical isomers of zeaxanthin, DMPC and 14-PC, are presented in Fig. 1.

2.2. Preparation of liposomes

The membranes used in this work were multilamellar dispersions of DMPC containing 1 mol% 14-PC and 10 mol% 9-*cis*, 13-*cis*, or all-*trans* zeaxanthin added to the sample during preparation. Briefly, these liposomes were prepared by the following method [23]: chloroform solutions of lipids, isomers of zeaxanthin, and 14-PC were mixed (containing ~ 0.5 μ mol of total lipids); the chloroform was evaporated with a stream of nitrogen gas; and the lipid film on the bottom of the test tube thoroughly dried under reduced pressure (about 0.1 mm Hg) for 12 h. Preheated buffer solution (0.25 ml of 10 mM PIPES and 150 mM NaCl, pH 7.0) was added to the dried film and vortexed at 40 °C for ~ 15 min. The multilamellar liposomes were centrifuged briefly (15 min at 4 °C with an Eppendorf bench centrifuge at 16,000 \times g), and the loose pellet (about 20% lipid, w/w) was used for EPR measurements.

2.3. Conventional EPR

For conventional EPR measurements, the sample was placed in a 0.6-mm i.d. capillary made of gas-permeable methylpentene polymer, called TPX, and the capillary was placed inside the EPR dewar insert. It was then equilibrated with nitrogen gas used for temperature control [28,29]. The sample was thoroughly deoxygenated. EPR spectra were obtained with an X-band Bruker EMX spectrometer with temperature-controlled accessories. Modulation amplitude of 0.5 G and an incident microwave power of 5.0 mW were used for measurement at 35 °C. To measure the hydrophobicity at the membrane center, the *z*-component of the hyperfine interaction tensor of the 14-PC, A_z , was determined from the EPR spectra of 14-PC for samples frozen at -163 °C, recorded with modulation amplitude of 2 G and an incident microwave power of 2 mW [30]. Fig. 2 shows the typical conventional EPR spectra of 14-PC in investigated membranes recorded at 35 °C and -163 °C with the indication of the measured spectral parameters.

2.4. Saturation recovery EPR

The spin-lattice relaxation times (T_{1s}) of the 14-PC were determined by analyzing the saturation recovery signal of the central line obtained by short-pulse saturation recovery EPR at X-band [31,32]. Accumulation of the saturation recovery signals was carried out with 2048 data points on each decay. Details for measurements with carotenoids are described in our earlier paper [33] (see also the caption to Fig. 3A).

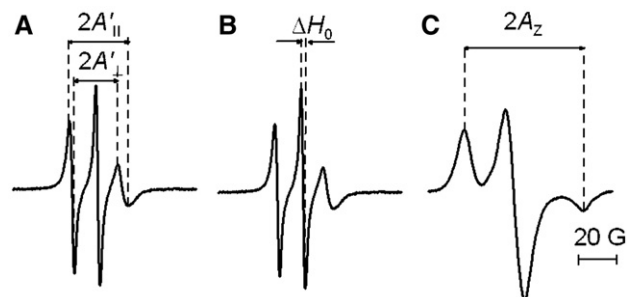


Fig. 2. EPR spectra of 14-PC in DMPC membranes containing 10 mol% 9-*cis* zeaxanthin recorded at 35 °C (A, B) and -163 °C (C). Measured values for evaluating order parameters ($A'_{||}$ and A'_{\perp}) are indicated in panel A. In panel B, the measured ΔH_0 value (peak-to-peak central line width) is indicated. In panel C, the measured $2A_z$ value (*z*-component of the hyperfine interaction tensor) is indicated.

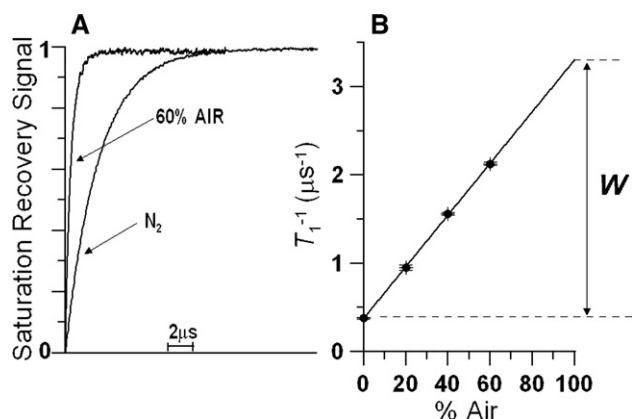


Fig. 3. (A) Representative saturation recovery signals of 14-PC in DMPC membranes containing 10 mol% 9-*cis* zeaxanthin at 35 °C for samples equilibrated at 35 °C with nitrogen gas and with a gas mixture of 60% air and 40% nitrogen. The fits to the single-exponential curves with recovery times of 2.64 μ s (N_2) and 0.47 μ s (60% air) were satisfactory. The decay time constant can be determined with the accuracy of $\pm 3\%$. (B) T_1^{-1} for 14-PC in DMPC membranes containing 10 mol% 9-*cis* zeaxanthin at 35 °C plotted as percent air in the equilibrating gas mixture. Experimental points show a linear dependence up to 60% air, and extrapolation to 100% is performed to indicate a way of calculating the oxygen transport parameters, W . The W values can be evaluated with the accuracy better than $\pm 10\%$.

In these experiments, the bimolecular collision rate between oxygen (a fast-relaxing species) and the nitroxide moiety of 14-PC (a slow-relaxing species) was evaluated in terms of an oxygen transport parameter ($W(x)$). $W(x)$ was defined as

$$W(x) = T_1^{-1}(\text{air}, x) - T_1^{-1}(N_2, x), \quad (1)$$

where the T_1 s are the spin-lattice relaxation times of the nitroxide in samples equilibrated with atmospheric air and nitrogen, respectively [34]. $W(x)$ is proportional to the product of the local translational diffusion coefficient $D(x)$ and the local concentration $C(x)$ of oxygen at a “depth” x in a lipid bilayer that is equilibrated in the atmospheric air (at C14 position in present experiments):

$$W(x) \sim D(x)C(x). \quad (2)$$

For measurements of the oxygen transport parameter, the concentration of oxygen in the sample was controlled by equilibration with the same gas that was used for the temperature control (i.e., a controlled mixture of nitrogen and dry air adjusted with flowmeters (Matheson Gas Products model 7631H-604) [28,29]) (see also Fig. 3B for more explanation).

3. Results

3.1. Saturation recovery measurements

To get more insight into the interactions of different isomers of zeaxanthin with the lipid bilayer in the bilayer center, we applied the saturation recovery spin label oximetry method, which is a dual-probe saturation recovery EPR approach in which the observable parameter is the spin-lattice relaxation time (T_1) of lipid spin labels and the measured value is the bimolecular collision rate between molecular oxygen and the nitroxide moiety of spin labels. This method has proven to be extremely sensitive to changes in the local oxygen diffusion-concentration product (around the nitroxide moiety) because of the long T_1 of lipid spin labels (1–10 μ s) and also because molecular oxygen is a unique probe molecule. Molecular oxy-

gen is paramagnetic, small, and has an appropriate level of hydrophobicity that allows it to enter the small vacant pockets that are transiently formed in the lipid bilayer membrane. Therefore, collision rates between molecular oxygen and nitroxide spin labels at specific locations in the membrane are sensitive to the dynamics of *gauche-trans* isomerization of lipid hydrocarbon chains and to the structural nonconformability on neighboring lipids [31,35–37]. The free volume in the lipid bilayer may be very small, just sufficient to contain a single molecule of oxygen. Kusumi et al. [34] concluded that the oxygen transport parameter (see Eq. (1)) is a useful monitor of membrane fluidity that reports on translational diffusion of small molecules. We used this parameter to monitor effects of different isomers of zeaxanthin in the central region of the DMPC bilayer.

Fig. 3A shows typical saturation recovery curves for 14-PC in the DMPC membrane containing 10 mol% 9-*cis* zeaxanthin at 35 °C in the presence and absence of oxygen. The recovery curves were fitted by single, double, and triple exponentials and compared. For all of the recovery curves obtained in this work, the results indicated that no substantial improvement in the fitting was observed when the number of exponentials was increased from one, suggesting that these recovery curves can be analyzed as single exponentials. The decay time constants were determined with an accuracy of $\pm 3\%$.

The spin-lattice relaxation times of 14-PC recorded for DMPC samples containing *cis*-isomers of zeaxanthin (in the absence of oxygen) were always significantly greater than the spin-lattice relaxation time recorded for the pure DMPC bilayer (without zeaxanthin). This result, in agreement with the theoretical development on spin-lattice relaxation of nitroxides [38], indicates that the translational motion of 14-PC is suppressed. In our earlier work [33], we showed that the macular xanthophyll lutein increases T_1 of lipid spin labels at all depths in the membranes, while cholesterol increases T_1 in and near the polar headgroup region and decreases it in the membrane center. The major conclusion from this work was that cholesterol increases frequency of chain bending in the membrane center, while lutein decreases this frequency. Comparison of the effects of xanthophylls and cholesterol in the membrane center should help to determine position and orientation of *cis*-isomers in the lipid bilayer (see also Discussion).

3.2. Oxygen transport parameter at the membrane center

Saturation recovery measurements were carried out systematically as a function of the partial pressure of oxygen in the equilibrating gas mixture for all investigated isomers of zeaxanthin present in the DMPC bilayer. Previously, we proved that lipid spin labels are able to partition between different membrane domains, and that the presence of two recovery constants in the saturation recovery curve (which indicates the presence of two membrane environments) can be found more readily in the presence of oxygen [32,35,39,40]. However, in this work, single exponential recovery was constantly observed, both in the absence and presence of oxygen. This indicates the presence of a single homogenous membrane when averaged

over 0.3 μs (the shortest recovery time observed here), and that, in the membranes, the rate of lipid exchange among the purported membrane domains is greater than the T_1 relaxation rate (greater than $3.3 \times 10^6 \text{ s}^{-1}$, see Refs. [32,35] for more details).

In Fig. 3B, T_1^{-1} values measured for 14-PC in the DMPC membranes containing 10 mol% 9-*cis* zeaxanthin at 35 °C are plotted as a function of oxygen concentration (in % air) in the equilibrating gas mixture. All plots of T_1^{-1} for investigated membranes show a linear dependence on the oxygen concentration between 0 and 60% air. For each sample, the oxygen transport parameter was obtained by extrapolating the linear plot to the sample equilibrated with atmospheric air (100% air, see Eq. (1)) as shown in Fig. 3B. This process is required because accurate observation of saturation recovery becomes increasingly difficult as the oxygen partial pressure is increased due to fast relaxations. Not less than three decay measurements were performed for each point in the plot with the accuracy of the evaluation of $W(x)$ better than $\pm 10\%$.

The oxygen transport parameter at 35 °C for DMPC membranes with and without the addition of 10 mol% isomers of zeaxanthin obtained using 14-PC spin labels are shown in Fig. 4. Significant decreases in $W(x)$ at the membrane center of the DMPC bilayer were induced by incorporating all of the isomers of zeaxanthin in the membrane. The strongest effect was observed for the 13-*cis* isomer, a weaker effect for the 9-*cis* isomer, and the weakest for the all-*trans* isomer. The very strong effect of *cis*-isomers on the oxygen transport parameter in the membrane center suggests that the investigated *cis*-isomers of zeaxanthin, similarly to the all-*trans* isomers, are located in the membrane center, adopting transmembrane orientation with the polar terminal hydroxyl groups anchored in the opposite leaflets of the bilayer. This was a rather unexpected result in light of the model appearing in the literature, which placed *cis*-isomers of zeaxanthin horizontally with respect to the plane of the membrane and with polar hydroxyl groups anchored in the same polar headgroup region (the same leaflet) of the bilayer (see [21,41]). Because of this we have undertaken additional measurements to see how these *cis*-isomers affect other membrane properties including alkyl chain order, fluidity, and hydrophobicity.

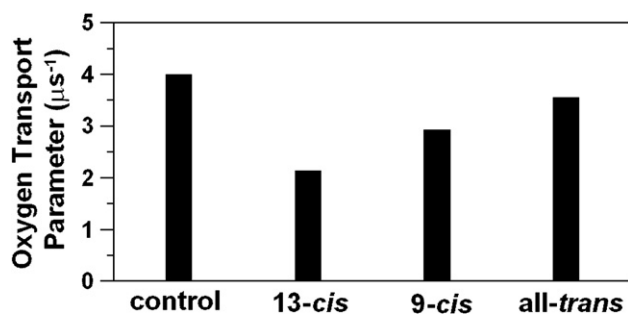


Fig. 4. The oxygen transport parameter measured at 35 °C with the use of 14-PC in the center of the pure DMPC membrane (Control) and DMPC membranes containing 10 mol% 13-*cis*, 9-*cis*, or all-*trans* isomer of zeaxanthin. The accuracy of the evaluation of the oxygen transport parameter is better than $\pm 10\%$.

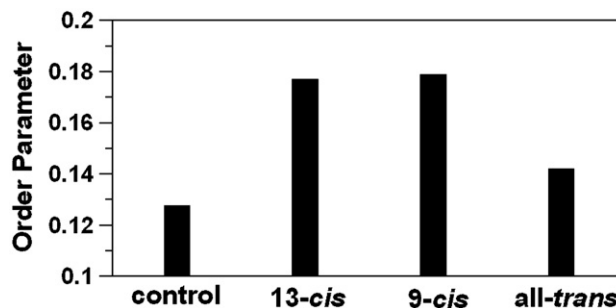


Fig. 5. Changes of the molecular order parameter of 14-PC in DMPC membranes induced by the addition of 10 mol% 13-*cis*, 9-*cis*, or all-*trans* isomer of zeaxanthin and measured at 35 °C. Control indicates order parameter measured without additions. Because of the sharpness of the EPR lines for 14-PC (see Fig. 2), A'_{\parallel} and A'_{\perp} values can be measured with the accuracy of $\pm 0.1 \text{ G}$, and the order parameter can be evaluated with the accuracy of ± 0.015 .

3.3. Order of membrane interior

One of the features of conventional EPR spectra of 14-PC for samples containing *cis*- and *trans*-isomers of zeaxanthin is that none show any indication of the presence of two components (weakly and strongly immobilized). We can conclude that zeaxanthin is well dispersed in the membrane on a time scale determined by the anisotropy of the hyperfine interaction of the nitroxide (10 ns). This result is consistent with the oxygen transport data, in which all of the saturation recovery curves were single-exponential curves. We should mention here that the use of a spin probe attached to the C14 position of the alkyl chain was first employed by Knowles et al. and Marsh et al. [42,43]. Their results indicate that the presence of two components in a conventional EPR spectrum is visually clearer with phospholipids labeled at C14 than at other positions in the alkyl chain.

Effects of 10 mol% geometrical isomers of zeaxanthin added to the sample on the order parameter of 14-PC are summarized in Fig. 5. The order parameter was calculated according to Marsh [44] from parameters measured directly from the EPR spectra as indicated in Fig. 2. It can be seen that the effect of *cis*-isomers of zeaxanthin is greater than the effect of the all-*trans* isomer. However, no significant difference in the effect of 9-*cis* and 13-*cis* zeaxanthin was indicated. Results presented in Fig. 5 confirm our conclusion made in Section 3.2 about transmembrane localization of *cis*-isomers of zeaxanthin in the DMPC bilayer.

In the membrane, the alkyl chain of 14-PC with the nitroxide moiety attached at the C14 position (see Fig. 1) undergoes rapid anisotropic motion about the long axis of the spin label and wobbling motion of the long axis within the confines of a cone imposed by the membrane environment. Increase in an order parameter indicates that the cone angle of the cone for the wobbling motion of the alkyl chain decrease. Because *cis*- and *trans*-isomers of zeaxanthin exert their effects by the steric contact with alkyl chains and introducing the “rigid walls” for wobbling motion, it can be inferred that the rigid, bar-like portion of both isomers is located in the membrane center. Thus, obtained results suggest that the investigated *cis*-isomers of

zeaxanthin, similarly to the all-*trans* isomer, are located in the membrane interior, adopting transmembrane orientation with the polar terminal hydroxyl groups located in the opposite leaflets of the bilayer.

3.4. Fluidity of membrane interior

Membrane fluidity can be evaluated directly from the EPR spectra of 16-PC (or 16-SASL) by measuring the effective rotational correlation time of the free radical moiety of this lipid spin label, assuming its isotropic rotational diffusion [45]. The rotational correlation time can be calculated from the linear and the quadratic term of the line width parameter. As was indicated in Ref. [45] the motional model is fairly good and the motion is isotropic when both calculated correlation times are similar and correlation time is smaller than 2 ns. Here we used 14-PC because of the best match with the thickness of the DMPC bilayer (14 carbon atoms in the hydrocarbon chain). The nitroxide moiety of 14-PC shows less motion in the DMPC bilayer than 16-PC, and evaluated rotational correlation times are close to 2 ns. Additionally, rotational correlation times evaluated from the linear and the quadratic term of the line width parameter are very different, which indicate onset of anisotropic motion and the invalidity of using the abovementioned model. Because of this we used the peak-to-peak width of the central line of the EPR spectrum as a conventional experimental parameter related to the rotational motion of the nitroxide moiety of 14-PC (see also Refs. [24,46] for the use of this parameter). Bigger peak-to-peak width indicates slower rotational motion. Fig. 6 shows the peak-to-peak line width of 14-PC in the DMPC bilayer in the absence and presence of 10 mol% geometrical isomers of zeaxanthin. All isomers increase the line width of the EPR spectrum, indicating that they not only decrease the cone angle of the cone inside of which wobbling motion occurs, but also decrease the rate of rotation inside the cone for flexible hydrocarbon chains. As in earlier observations, the effect of the 13-*cis* isomer is the greatest and the effect of the *trans*-isomer is the smallest.

We would like to point out that an order parameter indicates the static property of the lipid bilayer, whereas the rotational motion and the oxygen transport parameter characterize mem-

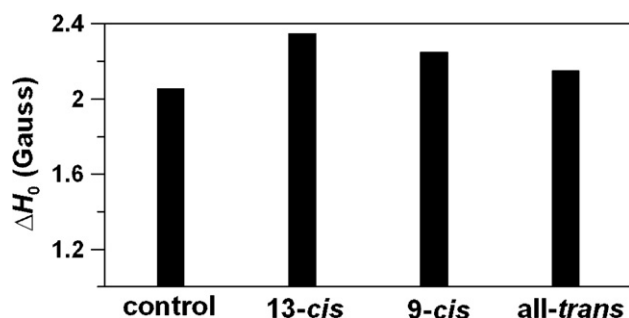


Fig. 6. Changes of the peak-to-peak central line width, ΔH_0 , of 14-PC in DMPC membranes induced by the addition of 10 mol% 13-*cis*, 9-*cis*, or all-*trans* isomer of zeaxanthin and measured at 35 °C. Control indicates ΔH_0 measured without additions. Because of the sharpness of the central EPR lines for 14-PC (see Fig. 2), the ΔH_0 value can be measured with the accuracy better than ± 0.05 G.

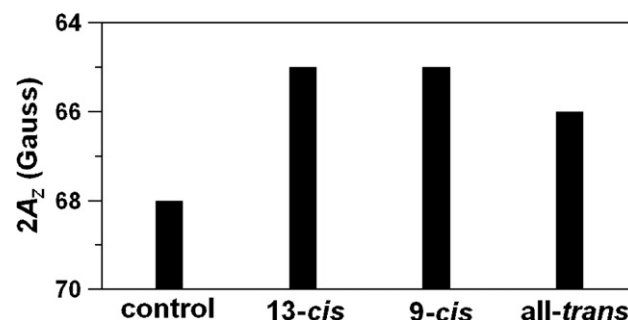


Fig. 7. A_z values (in Gauss) for DMPC membranes in the absence and presence of 10 mol% 13-*cis*, 9-*cis*, or all-*trans* isomer of zeaxanthin measured with 14-PC. Taller bars indicate higher hydrophobicity. $2A_z$ values can be measured with the accuracy of ± 0.25 G.

brane dynamics (membrane fluidity) that report on rotational diffusion of alkyl chains and translational diffusion of oxygen molecules, respectively. The EPR spin-labeling approach also makes it possible to monitor another bulk property of the lipid bilayer membrane, namely local membrane hydrophobicity.

3.5. Hydrophobicity of membrane interior

To compare effects of 9-*cis* and 13-*cis* isomers of zeaxanthin with the all-*trans* isomer on the hydrophobicity of the membrane center, we used, as a conventional parameter, the z -component of the hyperfine interaction tensor (A_z) of 14-PC [23,30]. With the increase of the local hydrophobicity around the nitroxide moiety of 14-PC, A_z decreases. Results presented in Fig. 7 indicate that all isomers significantly increase the hydrophobicity of the membrane interior, with the effects of *cis*-isomers being greater than those of the *trans*-isomer. The difference between the effects of 9-*cis* and 13-*cis* isomers is negligible. Usually, we relate the local hydrophobicity in the lipid bilayer as observed by A_z to the hydrophobicity (or ϵ) of bulk organic solvent by referring to Fig. 2 in Ref. [30]. After addition of 10 mol% zeaxanthin the hydrophobicity of the DMPC membrane center increases from the level close to that of 2-propanol ($\epsilon \approx 20$) for pure DMPC to the level close to that of 1-decanol and ethyl acetate ($\epsilon \approx 6$ –9) for *trans*-zeaxanthin, and to the level close to that of dipropylamine and *N*-butylamine ($\epsilon \approx 3$ –4) for 9-*cis* and 13-*cis* zeaxanthin. The induced increase of hydrophobicity is significant, causing decrease of the dielectric constant from the value of ~ 20 to close to 3. Griffith et al. [47,48] demonstrated that the hydrophobicity in the membrane interior is largely determined by the extent of water penetration into the membrane, since the dehydration abolishes the hydrophobicity gradient in liposome samples. The greater effect of the *cis*-isomers in the membrane center is probably a result of the introduction of a larger number of conjugated double bonds into that region (due to their bent structure), as compared with the *trans*-isomer (see Fig. 1 and scheme presented in Fig. 8). Lipid bilayers containing unsaturated alkyl chains (double bonds) demonstrate less water penetration into the hydrocarbon region than saturated bilayers [30,49]. It is also known that unsaturated hydrocarbons are less hygroscopic than saturated hydrocarbons.

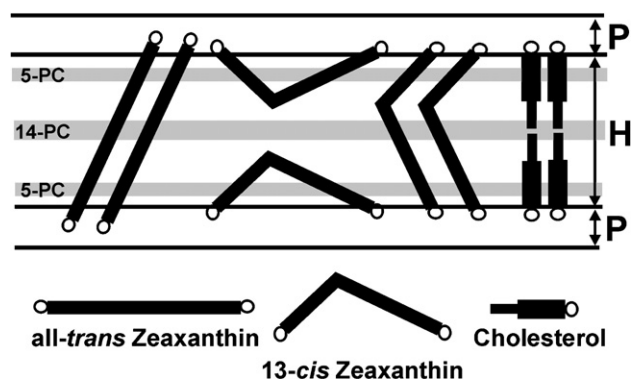


Fig. 8. A schematic drawing of the localization of different isomers of zeaxanthin in the DMPC bilayer. The horizontally orientated *cis*-isomers of zeaxanthin should create more vacant pockets in the membrane center and increase membrane dynamics in that region. Their effects should be very similar to those caused by cholesterol molecules. The transmembrane orientated *cis*-isomers of zeaxanthin should decrease membrane dynamics in the membrane center. Their effects should be very similar to those caused by all-*trans* zeaxanthin. Hatched areas indicate regions of the membrane probed by 14-PC and 5-PC.

In our earlier paper, we showed that the *trans*-isomers of dipolar xanthophylls increase the hydrophobicity of the saturated membrane interior and the effect monitored in the membrane center is independent of the membrane thickness [23]. However, the effects in and near the polar headgroup regions strongly depend on the membrane thickness, more strictly, on its relation to the length of the xanthophyll molecule (distance between the polar hydroxyl groups at both ends of the molecule). In thin membranes (DLPC, DMPC), these dipolar xanthophylls are tilted with respect to the bilayer normal [10,23,24]. In thick membranes (DSPC, DBPC), the polar groups of dipolar xanthophylls sink deeper into the hydrocarbon region, preserving, however, their transmembrane orientation (for DBPC, see Ref. [24]). In our present work, the thickness of the bilayer is fixed (the same DMPC was used in all measurements); however, the distance between the polar hydroxyl groups in different xanthophyll isomers decreases as all-*trans* > 9-*cis* > 13-*cis*. We think the above explanation should also be valid in this case, supporting our conclusion about transmembrane orientation of *cis*-isomers in the lipid bilayer.

3.6. Effects at C5 position

The amount of available *cis*-isomers of zeaxanthin was very limited; however, we were able to perform a few measurements at a depth close to the membrane surface. We measured effects of the inclusion 10 mol% 13-*cis* isomer of zeaxanthin on the order, hydrophobicity, and oxygen transport parameter at the C5 position in fluid phase DMPC membranes with the use of 5-PC spin label. Observed effects were compared with those caused by the all-*trans* isomer of zeaxanthin. Both isomers increased alkyl chain order and hydrophobicity, and decreased the oxygen transport parameter (data not shown). The effects caused by the 13-*cis* isomer were greater than those caused by the all-*trans* isomer. Obtained results can be explained by the transmembrane and/or horizontal orientation of the 13-*cis* isomer of zeaxanthin in the DMPC bilayer. At the transmembrane orien-

tation, both ends of the 13-*cis* isomer should sink deeper into the lipid bilayer and ionone rings should be closer to the nitroxide at the C5 position, strongly influencing lipid bilayer properties at this depth. In a similar way, the all-*trans* xanthophylls affected properties of thick membranes at C5 position more strongly than property of thin membranes because ionone rings sink deeper in thick membranes [23,24]. It is also probable that at the horizontal orientation, when the 13-*cis* zeaxanthin molecule is located in one leaflet and anchored by the terminal hydroxyl groups at the same polar headgroup region, the effect of the 13-*cis* isomer on membrane properties measured at the C5 position is stronger than the effect of the *trans*-isomer. As expected, measurements at the C5 position cannot distinguish between these two orientations of *cis*-zeaxanthin molecules.

4. Discussion

Previously, we investigated the interaction of *trans*-isomers of xanthophylls (including *trans*-zeaxanthin) with model membranes, looking at alkyl chain order and rotational motion, membrane phase transition, and hydrophobicity of the membrane interior [22–26,33,50]. Our results were in principal agreement with those obtained for biological membranes [51–53]. In our investigations, special attention was paid to the effects of carotenoids on the profiles of the oxygen transport parameter across the lipid bilayer [25,50]. We have also investigated the same membrane properties in the presence of cholesterol [30,31,33,36,39,54,55]. This work has shown that the effects of *trans*-xanthophylls (*trans*-zeaxanthin) on the structure and dynamics of lipid bilayer membranes are similar to the effects of cholesterol in many aspects. Both increase the order and decrease the alkyl chain motion (observed with a conventional EPR spin-labeling method) in fluid-phase membranes and both are known to broaden the gel-to-fluid phase transition and increase the mobility of polar head groups. As a rule, the presence of unsaturated alkyl chains moderates the effect of *trans*-xanthophylls and cholesterol. A quantity of 10 mol% *trans*-isomers of dipolar xanthophylls added to the sample exerts an effect similar to that of 15–20 mol% cholesterol. Both modifiers also increase the hydrophobicity of the membrane center. However, *trans*-isomers of dipolar xanthophylls decrease the oxygen transport parameter (oxygen diffusion-concentration product) in saturated and unsaturated membranes, with the effect strongest in the membrane center [25,50], whereas cholesterol does not change or increase the oxygen transport parameter in the membrane center [31,36,39,55]. Furthermore, *trans*-isomers of dipolar xanthophylls decrease the frequency of alkyl chain bending, with the effect strongest in the membrane center, whereas cholesterol decreases this frequency near the polar headgroup region and increases it in the membrane center [33]. These effects are manifested not only by changes in frequency of bimolecular collisions between spin label pairs, but also by changes in the spin-lattice relaxation time of spin labels. Dipolar xanthophylls in all-*trans* conformations increase the T_1 of spin labels in the membrane center, while cholesterol decreases it.

The observed differences in the effects of these modifiers result from differences in the structure of all-*trans* dipolar

xanthophylls and cholesterol and from their different locations within the lipid bilayer membrane (see Figs. 1 and 8). The cholesterol molecule is located in one leaflet of the bilayer, and its rigid plate-like portion extends to the depth of the 7th to 10th carbon atom in a lipid hydrocarbon chain [56]. The cross-section of the isooctyl chain of the cholesterol molecule is much smaller than the cross-section of the rigid steroid ring and, therefore, produces additional possibilities for undulation and *trans-gauche* transitions of alkyl chains in the membrane center. Thus, the cholesterol molecule creates many vacant pockets in the membrane center that oxygen molecules can occupy, jumping from one pocket to an adjacent one or moving with the movement of the pocket itself due to the rapid *gauche-trans* isomerization of the phospholipid hydrocarbon chains. In contrast, one dipolar carotenoid molecule influences both halves of the lipid bilayer. With two polar groups interacting with opposite hydrophilic regions of the membrane, this molecule can brace together the two halves of the bilayer like a tie bar [52]. Therefore, both – the oxygen transport parameter and vertical fluctuations of the ends of alkyl chains – are reduced in those regions of the lipid bilayer membranes to which the rigid portion of molecule of the modifier extends (see scheme in Fig. 8).

In our present work, using one spectroscopic technique but different approaches, we were able to obtain a vast amount of information from one membrane location, in this case from the membrane center (C14 position). As indicated above, this position is the most significant if we choose to distinguish between two orientations of *cis*-isomers of zeaxanthin in the lipid bilayer membrane. If the most accepted model, the horizontal orientation of *cis*-isomers, is correct [21,41], the effects observed in the membrane center should be similar to those observed for cholesterol molecules. If the transmembrane orientation is prevalent, the effects of *cis*-isomers should be similar to those caused by the *trans*-zeaxanthin (see scheme in Fig. 8). Effects observed in membrane regions closer to the membrane surface should be similar for both orientations of the *cis*-isomers of zeaxanthin. We should mention here that we are measuring averaged effects from both membrane leaflets.

Present results clearly showed that effects of *cis*-isomers of zeaxanthin on all investigated membrane properties observed in the membrane center and near the polar headgroup region are similar to those caused by the *trans*-isomer. However, effects of *cis*-isomers, observed in the membrane center, on the oxygen transport parameter and T_1 value of 14-PC are very different from those caused by cholesterol. This allowed us to conclude that most molecules of *cis*-isomers adopt transmembrane orientation, similar to that adopted by molecules of the *trans*-isomer. Unexpectedly, effects of *cis*-isomers were greater than those caused by the *trans*-isomer. Similar observations were made by Kostecka-Gugola A., Milanowska J., Gruszecki W. I., and Strzalka K. (personal communication), who also detected greater effects of 9-*cis* and 13-*cis* isomers of zeaxanthin on thermodynamic characteristics of the main phase transition of the DPPC membrane, measured with the differential scanning calorimetry, than effects caused by the all-*trans* isomer. This can be explained by the fact that the rigid hydrocarbon portion of transmembrane oriented *cis*-isomers is tilted with respect to the membrane

normal (see Fig. 8), and/or that *cis*-isomers are better soluble in the lipid bilayer than *trans*-isomers (they do not form higher aggregates).

It was shown that all-*trans* isomers of dipolar xanthophylls affect the properties of thin membranes (DLPC, DMPC) more strongly than the properties of thick membranes (DPPC, DSPC, DBPC) [22,24], presumably because in thin membranes these dipolar xanthophylls are tilted with respect to the bilayer normal [10,57–60] and interact with the larger number of alkyl chains. Thus, the effect of the tilted *cis*-isomer should be stronger than the effect of the less tilted *trans*-isomer. However, we should mention here that in the DMPC bilayer *trans*-zeaxanthin is tilted by $\sim 25^\circ$ [10], which somewhat weakens our explanation. Our second explanation was based on the statement that dipolar xanthophylls should affect membrane properties mainly when they are dissolved in the lipid bilayer as monomers. The reported threshold of the solubility for all-*trans* xanthophylls in lipid membranes is ~ 10 mol% [61]; however, lower and higher values were also indicated (see Discussion in Ref. [22]). Organization of *cis*-zeaxanthin in the membrane is less investigated. We can, however, make some conclusions based on measurements with monomolecular layers on the air–water interface formed from the mixture of DPPC and all-*trans*, 9-*cis*, or 13-*cis* zeaxanthin [41,62]. Authors of these papers showed that the concentration of zeaxanthin in the monomolecular layer at which aggregation starts is ~ 5 mol% for *trans*, ~ 20 mol% for 9-*cis*, and higher than 20 mol% for 13-*cis* zeaxanthin. Additionally, *cis*-isomers of zeaxanthin do not show a tendency to organize into higher aggregates, even in a very polar solvent like ethanol/water mixture (5:95 v/v), where the *trans*-isomers aggregate easily [41]. Having in mind the above discussion, we can argue that the later explanation is more probable.

The transmembrane orientation of the *cis*-isomers of zeaxanthin is probably enhanced in thin lipid bilayer membranes in which the thickness of the hydrophobic core is smaller than the distance between the hydroxyl groups at the 3 and 3' positions of zeaxanthin. The thicknesses of the hydrocarbon region in the fluid-phase DMPC bilayer (H in Fig. 8) and the polar headgroup and glycerol backbone region (P in Fig. 8) are 24.4 Å and 5.3 Å, respectively (see Ref. [63] for the evaluation these thicknesses). The distances between polar hydroxyl groups (O–O) in different geometrical isomers of zeaxanthin were obtained using molecular modeling techniques and were provided to us by Ewa Borcowska, a PhD student of Dr. Marta Pasenkiewicz-Gierula. They are as follows: 30.52 Å for all-*trans*, 26.86 Å for 9-*cis*, and 24.38 Å for 13-*cis*. Thus, all isomers are able to span the hydrophobic core of the DMPC membrane. However, in thick membranes, the horizontal orientation of the *cis*-isomers may be prevalent.

We would like to add that conventional EPR spectra as well as saturation recovery curves measured in both the presence and absence of molecular oxygen showed that 14-PC detects the existence of a single homogenous environment, indicating that both carotenoids and DMPC are likely to be undergoing fast translational diffusion in DMPC/zeaxanthin membranes. If the zeaxanthin reach domains are formed, the lipid exchange rates

between these purported regions should be faster than 10 ns (time scale determined by the anisotropy of the hyperfine interaction of the nitroxide), and/or these regions must be forming and dispersing rapidly on a time scale shorter than 0.3 μ s (the shortest spin-lattice relaxation time measured in the presence of oxygen). Although, this does not exclude the possibility of the formation of small, stable aggregates of zeaxanthin (see discussion above).

Acknowledgments

This work was supported by grants EY015526, EB002052, and EB001980 of the National Institutes of Health.

References

- [1] Y. Koyama, I. Takatsuka, M. Kanaji, K. Tomimoto, M. Kuro, T. Shimamura, J. Ymashita, K. Saiki, K. Tsukida, Configurations of carotenoids in the reaction center and the light-harvesting complex of *Rhodospirillum rubrum*. Natural selection of carotenoid configurations by pigment protein complexes, *Photochem. Photobiol.* 51 (1990) 119–128.
- [2] F. Bouvier, A. D'harlingue, R.A. Backhaus, M.H. Kumagai, B. Camara, Identification of neoxanthin synthase as a carotenoid cyclase paralog, *Eur. J. Biochem.* 267 (2000) 6346–6352.
- [3] N.I. Krinsky, M.M. Russett, G.J. Handelman, D.M. Sondderly, Structural and geometrical isomers of carotenoids in human plasma, *J. Nutr.* 120 (1990) 1654–1662.
- [4] F. Khachik, C.J. Spangler, J.C. Smith Jr., L.M. Canfield, A. Steck, H. Pfander, Identification, quantification, and relative concentrations of carotenoids and their metabolites in human milk and serum, *Anal. Chem.* 69 (1997) 1873–1881.
- [5] W. Stahl, W. Schwarz, J. Von Laar, H. Sies, All-*trans* β -carotene preferentially accumulates in human chylomicrons and very low density lipoproteins compared with the 9-*cis* geometrical isomers, *J. Nutr.* 125 (1995) 2128–2133.
- [6] J.W. Ederman Jr., A.J. Thatcher, N.E. Hofmann, J.D. Lederman, S.S. Block, C.M. Lee, S. Mokady, All-*trans* beta-carotene is absorbed preferentially to 9-*cis* beta-carotene but the latter accumulates in the tissues of domestic ferrets (*Mustela putorius puro*), *J. Nutr.* 128 (1998) 2009–2013.
- [7] A.C. Boileau, N.R. Merchen, K. Wasson, C.A. Atkinson, J.W. Ederman Jr., *cis*-Lycopene is more bioavailable than *trans*-lycopene *in vitro* and *in vivo* in lymph-cannulated ferrets, *J. Nutr.* 129 (1999) 1176–1181.
- [8] W. Stahl, W. Schwarz, A.R. Saundquist, H. Sies, *cis-trans* Isomers of lycopene and beta-carotene in human serum and tissues, *Arch. Biochem. Biophys.* 294 (1992) 173–177.
- [9] D. Max Sondderly, M.D. Russett, R. Land, N.I. Krinsky, Plasma carotenoids of monkeys (*Macaca fascicularis* and *Saimiri sciureus*), *J. Nutr.* 120 (1990) 1663–1671.
- [10] W.I. Gruszecki, J. Sielewiesiuk, Orientation of xanthophylls in phosphatidylcholine multibilayer, *Biochim. Biophys. Acta* 1023 (1990) 405–412.
- [11] A. Sujak, J. Gabrielska, W. Grudziński, R. Bore, P. Mazurek, W.I. Gruszecki, Lutein and zeaxanthin as protectors of lipid membranes against oxidative damage: the structural aspects, *Arch. Biochem. Biophys.* 371 (1999) 301–307.
- [12] R.A. Bone, J.T. Landrum, Macular pigment in Henle fiber membranes: a model for Haidinger's brushes, *Vis. Res.* 24 (1984) 103–108.
- [13] R.A. Bone, J.T. Landrum, A. Cains, Optical density spectra of the macular pigment in vivo and in vitro, *Vis. Res.* 32 (1992) 105–110.
- [14] R.A. Bone, J.T. Landrum, Dichroism of lutein: a possible basis for Haidinger's brushes, *Appl. Opt.* 22 (1983) 775–776.
- [15] W.I. Gruszecki, A. Sujak, K. Strzalka, A. Radunz, G.H. Schmid, Organisation of xanthophyll-lipid membranes studied by means of specific pigment antisera, spectrophotometry and monomolecular layer technique: lutein versus zeaxanthin, *Z. Naturforsch., C* 54 (1999) 517–525.
- [16] W. Okulski, A. Sujak, W.I. Gruszecki, Dipalmitoylphosphatidylcholine membranes modified with zeaxanthin: numeric study of membrane organization, *Biochim. Biophys. Acta* 1509 (2000) 216–228.
- [17] R.A. Bone, J.T. Landrum, G.W. Hime, A. Cains, Stereochemistry of the human macular carotenoids, *Invest. Ophthalmol. Vis. Sci.* 34 (1993) 2033–2040.
- [18] J.T. Landrum, R.A. Bone, Lutein, zeaxanthin, and the macular pigment, *Arch. Biochem. Biophys.* 385 (2001) 28–40.
- [19] P.S. Bernstein, F. Khachik, L.S. Carvalho, J.M. Garth, Z. Da-You, N.B. Katz, Identification and quantitation of carotenoids and their metabolites in the tissues of human eye, *Exp. Eye Res.* 72 (2001) 215–223.
- [20] N.I. Krinsky, Possible biologic mechanisms for protective role of xanthophylls, *J. Nutr.* 132 (2002) 540S–542S.
- [21] W.I. Gruszecki, Carotenoid orientation: role in membrane stabilization, in: N.I. Krinsky, S.T. Mayne, H. Sies (Eds.), *Carotenoids in Health and Disease*, Marcel Dekker, New York, 2004, pp. 151–163.
- [22] A. Wisniewska, J. Widomska, W.K. Subczynski, Carotenoid-membrane interactions in liposomes: effect of dipolar, monopolar, and nonpolar carotenoids, *Acta Biochim. Pol.* 53 (2006) 475–484.
- [23] A. Wisniewska, W.K. Subczynski, Effects of polar carotenoids on the shape of the hydrophobic barrier of phospholipid bilayers, *Biochim. Biophys. Acta* 1368 (1998) 235–246.
- [24] W.K. Subczynski, E. Markowska, J. Sielewiesiuk, Spin-label studies on phosphatidylcholine-polar carotenoid membranes: effects of alkyl chain length and unsaturation, *Biochim. Biophys. Acta* 1150 (1993) 173–181.
- [25] W.K. Subczynski, E. Markowska, J. Sielewiesiuk, Effect of polar carotenoids on the oxygen diffusion-concentration product in lipid bilayers. An EPR spin label study, *Biochim. Biophys. Acta* 1068 (1991) 68–72.
- [26] W.K. Subczynski, E. Markowska, W.I. Gruszecki, J. Sielewiesiuk, Effects of polar carotenoids on dimyristoylphosphatidylcholine membranes: spin-label studies, *Biochim. Biophys. Acta* 1105 (1992) 97–108.
- [27] P. Molnar, J. Szablocs, (Z/E)-Photoisomerization of C40-carotenoids by iodine, *J. Chem. Soc., Perkin Trans. 2* (1993) 261–266.
- [28] J.S. Hyde, W.K. Subczynski, Spin-label oximetry, in: L.J. Berliner, J. Reuben (Eds.), *Biological Magnetic Resonance, Spin Labeling: Theory and Applications*, vol. 8, Plenum Press, New York, 1989, pp. 399–425.
- [29] W.K. Subczynski, C.C. Felix, C.S. Klug, J.S. Hyde, Concentration by centrifugation for gas exchange EPR oximetry measurements with loop-gap resonators, *J. Magn. Reson.* 176 (2005) 244–248.
- [30] W.K. Subczynski, A. Wisniewska, J.-J. Yin, J.S. Hyde, A. Kusumi, Hydrophobic barriers of lipid bilayer membranes formed by reduction of water penetration by alkyl chain unsaturation and cholesterol, *Biochemistry* 33 (1994) 7670–7681.
- [31] W.K. Subczynski, J.S. Hyde, A. Kusumi, Oxygen permeability of phosphatidylcholine-cholesterol membranes, *Proc. Natl. Acad. Sci. U. S. A.* 86 (1989) 4474–4478.
- [32] K. Kawasaki, J.-J. Yin, W.K. Subczynski, J.S. Hyde, A. Kusumi, Pulse EPR detection of lipid exchange between protein-rich raft and bulk domains in the membrane: methodology development and its application to studies of influenza viral membrane, *Biophys. J.* 80 (2001) 738–748.
- [33] J.-J. Yin, W.K. Subczynski, Effect of lutein and cholesterol on alkyl chain bending in lipid bilayers: a pulse electron paramagnetic resonance spin labeling study, *Biophys. J.* 71 (1996) 832–839.
- [34] A. Kusumi, W.K. Subczynski, J.S. Hyde, Oxygen transport parameter in membranes as deduced by saturation recovery measurements of spin-lattice relaxation times of spin labels, *Proc. Natl. Acad. Sci. U. S. A.* 79 (1982) 1854–1858.
- [35] I. Ashikawa, J.-J. Yin, W.K. Subczynski, T. Kouyama, J.S. Hyde, A. Kusumi, Molecular organization and dynamics in bacteriorhodopsin-rich reconstituted membranes: discrimination of lipid environments by the oxygen transport parameter using a pulse ESR spin-labeling technique, *Biochemistry* 33 (1994) 4947–4952.
- [36] W.K. Subczynski, J.S. Hyde, A. Kusumi, Effect of alkyl chain unsaturation and cholesterol intercalation on oxygen transport in membranes: a pulse ESR spin labeling study, *Biochemistry* 30 (1991) 8578–8590.
- [37] R.J. Pace, S.I. Chan, Molecular motions in lipid bilayers: III. Lateral and transversal diffusion in bilayers, *J. Chem. Phys.* 76 (1982) 4241–4247.

- [38] B.H. Robinson, D.A. Hass, C. Mailer, Molecular dynamics in liquid: spin lattice relaxation of nitroxide spin labels, *Science* 263 (1994) 490–493.
- [39] W.K. Subczynski, A. Wisniewska, J.S. Hyde, A. Kusumi, Three-dimensional dynamic structure of the liquid-ordered domain in lipid membranes as examined by pulse-EPR oxygen probing, *Biophys. J.* 92 (2007) 1573–1584.
- [40] W.K. Subczynski, J. Widomska, A. Wisniewska, A. Kusumi, Saturation-recovery electron paramagnetic resonance discrimination by oxygen transport (DOT) method for characterizing membrane domains, in: T.J. McIntosh (Ed.), *Methods in Molecular Biology, Lipid Rafts*, vol. 398, Humana Press, Totowa, 2007, pp. 143–157.
- [41] J. Milanowska, A. Polit, Z. Wasylewski, W.I. Gruszecki, Interaction of isomeric forms of xanthophyll pigment zeaxanthin with dipalmitoylphosphatidylcholine studied in monomolecular layers, *J. Photochem. Photobiol., B Biol.* 72 (2003) 1–9.
- [42] P.F. Knowles, A. Watts, D. Marsh, Spin-label studies of lipid immobilization in dimyristoylphosphatidylcholine-substituted cytochrome oxidase, *Biochemistry* 18 (1979) 4480–4487.
- [43] D. Marsh, A. Watts, R. Pates, R. Uhl, P.F. Knowles, M. Esmann, ESR spin label studies of lipid–protein interaction in membranes, *Biochem. J.* 37 (1982) 265–274.
- [44] D. Marsh, Electron spin resonance: spin labels, in: E. Grell (Ed.), *Membrane Spectroscopy*, Springer-Verlag, Berlin, 1981, pp. 51–142.
- [45] L.J. Berliner, Spin labeling in enzymology: spin-labeled enzymes and proteins. Rotational correlation times calculation, *Methods Enzymol.* 49 (1978) 466–470.
- [46] S. Pistolessi, R. Pogni, J.B. Feix, Membrane insertion and bilayer perturbation by antimicrobial peptide CM15, *Biophys. J.* 93 (2007) 1651–1660.
- [47] O.H. Griffith, P.J. Dehlinger, S.P. Van, Shape of the hydrophobic barrier of phospholipids bilayers (evidence for water penetration into biological membranes), *J. Membr. Biol.* 15 (1974) 159–192.
- [48] O.H. Griffith, P.C. Jost, Lipid spin labels in biological membranes, in: L.J. Berliner (Ed.), *Spin Labeling. Theory and Application*, Academic Press, New York, 1976, pp. 453–523.
- [49] T. Hiff, L. Kevan, Electron spin echo modulation studies of doxylstearic acid spin probes in frozen vesicles: interaction of the spin probe with water-d₂ and effects of cholesterol addition, *J. Phys. Chem.* 93 (1989) 1572–1575.
- [50] W.K. Subczynski, E. Markowska, Effect of carotenoids on oxygen transport within and across model membranes, *Curr. Top. Biophys.* 16 (1992) 62–68.
- [51] L. Huang, A. Haug, Regulation of membrane lipid fluidity in *Acholeplasma-laidlawii* — effect of carotenoid pigment content, *Biochim. Biophys. Acta* 352 (1974) 361–370.
- [52] M. Rohmer, P. Bouvier, G. Ourisson, Molecular evolution of biomembranes: structural equivalents and phylogenetic precursors of sterols, *Proc. Natl. Acad. Sci. U. S. A.* 76 (1979) 847–851.
- [53] W.I. Gruszecki, K. Strzalka, Does the xanthophyll cycle take part in the regulation of fluidity of the thylakoid membrane, *Biochim. Biophys. Acta* 1060 (1991) 310–314.
- [54] A. Kusumi, W.K. Subczynski, M. Pasenkiewicz-Gierula, J.S. Hyde, H. Merkle, Spin-label studies on phosphatidylcholine-cholesterol membranes: effects of alkyl chain length and unsaturation in the fluid phase, *Biochim. Biophys. Acta* 854 (1986) 307–317.
- [55] J. Widomska, M. Raguz, J. Dillon, E.R. Gaillard, W.K. Subczynski, Physical properties of the lipid bilayer membrane made of calf lens lipids: EPR spin labeling studies, *Biochim. Biophys. Acta* 1768 (2007) 1454–1465.
- [56] T.J. McIntosh, The effect of cholesterol on the structure of phosphatidylcholine bilayers, *Biochim. Biophys. Acta* 513 (1978) 43–58.
- [57] W.I. Gruszecki, J. Siewiesiuk, Galactolipide multibilayers modified with xanthophylls: orientational and diffractometric studies, *Biochim. Biophys. Acta* 1069 (1991) 21–26.
- [58] W.I. Gruszecki, A. Smal, D. Szymczuk, The effect of zeaxanthin on the thickness of dimyristoylphosphatidylcholine bilayer: X-ray diffraction study, *J. Biol. Phys.* 18 (1992) 271–280.
- [59] A. Sujak, P. Mazurek, W.I. Gruszecki, Xanthophyll pigments lutein and zeaxanthin in lipid multibilayers formed with dimyristoylphosphatidylcholine, *J. Photochem. Photobiol., B Biol.* 68 (2002) 39–44.
- [60] M. Suwasky, P. Hidalgo, K. Strzalka, A. Kostecka-Gugala, Comparative X-ray studies on the interaction of carotenoids with model phosphatidylcholine membranes, *Z. Naturforsch., C* 57 (2002) 129–134.
- [61] J. Gabrielska, W.I. Gruszecki, Zeaxanthin (dihydroxy- β -carotene) but not β -carotene rigidifies lipid membranes: a ¹H-NMR study of carotenoid-egg phosphatidylcholine liposomes, *Biochim. Biophys. Acta* 1285 (1996) 167–174.
- [62] A. Sujak, W.I. Gruszecki, Organization of zeaxanthin and lutein in two-component monomolecular layers in dipalmitoylphosphatidylcholine, *J. Photochem. Photobiol., B Biol.* 59 (2000) 42–47.
- [63] J. Widomska, M. Raguz, W.K. Subczynski, Oxygen permeability of the lipid bilayer membrane made of calf lens lipids, *Biochim. Biophys. Acta* 836 (in press), doi:10.1016/j.bbmem.2007.06.018.